



# Stable-isotopic anomalies and the accretionary assemblage of the Earth and Mars: A subordinate role for carbonaceous chondrites

Paul H. Warren\*

*Institute of Geophysics and Planetary Physics, University of California, Los Angeles, CA 90095–1567, United States*

## ARTICLE INFO

### Article history:

Received 9 June 2011

Received in revised form 30 August 2011

Accepted 31 August 2011

Available online 5 October 2011

Editor: R.W. Carlson

### Keywords:

carbonaceous chondrites  
bulk compositions (of planets)  
oxygen isotopes  
Ti isotopes  
Cr isotopes  
Fe isotopes

## ABSTRACT

Plots such as  $\epsilon^{54}\text{Cr}$  vs.  $\epsilon^{50}\text{Ti}$  and  $\epsilon^{54}\text{Cr}$  vs.  $\Delta^{17}\text{O}$  reveal a fundamental dichotomy among planetary materials. The “carbonaceous” chondrites, by virtue of high  $\epsilon^{50}\text{Ti}$  and high  $\epsilon^{62}\text{Ni}$ , as well as, especially for any given  $\Delta^{17}\text{O}$ , high  $\epsilon^{54}\text{Cr}$ , are separated by a wide margin from all other materials. The significance of the bimodality is further manifested by several types of meteorites with petrological-geochemical characteristics that suggest membership in the opposite category from the true pedigree as revealed by the stable isotopes. Ureilites, for example, despite having diversely low  $\Delta^{17}\text{O}$  and about the same average carbon content as the most C-rich carbonaceous chondrite, have clear stable-isotopic signatures of noncarbonaceous pedigree. The striking bimodality on the  $\epsilon^{54}\text{Cr}$  vs.  $\epsilon^{50}\text{Ti}$  and  $\epsilon^{54}\text{Cr}$  vs.  $\Delta^{17}\text{O}$  diagrams suggests that the highest taxonomic division in meteorite/planetary classification should be between carbonaceous and noncarbonaceous materials. The bimodality may be an extreme manifestation of the effects of episodic accretion of early solids in the protoplanetary nebula. However, an alternative, admittedly speculative, explanation is that the bimodality corresponds to a division between materials that originally accreted in the outer solar system (carbonaceous) and materials that accreted in the inner solar system (noncarbonaceous). In any event, both the Earth and Mars plot squarely within the noncarbonaceous composition-space. Applying the lever rule to putative mixing lines on the  $\epsilon^{50}\text{Ti}$  vs.  $\epsilon^{54}\text{Cr}$  and  $\Delta^{17}\text{O}$  vs.  $\epsilon^{54}\text{Cr}$  diagrams, the carbonaceous/(carbonaceous + noncarbonaceous) mixing ratio  $C/(C+NC)$  is most likely close to (very roughly) 24% for Earth and 9% for Mars. Estimated upper limits for  $C/(C+NC)$  are 32% for Earth and 18% for Mars. However, the uncertainties are such that isotopic data do not require or even significantly suggest that Earth has higher  $C/(C+NC)$  than Mars. Among known chondrite groups, EH yields a relatively close fit to the stable-isotopic composition of Earth.

© 2011 Elsevier B.V. All rights reserved.

## 1. Introduction

In modeling compositional relationships among meteorites and the terrestrial planets (Richter et al., 2006), an important issue is the role of carbonaceous chondrites. Many models of the bulk Earth and Mars compositions draw analogies with carbonaceous chondrites. For the Earth, Allège et al. (2001) and Palme and O'Neill (2004) (cf. McDonough and Sun, 1995) have argued that the Earth's volatile depletion trend is matched more closely by carbonaceous chondrites than by any known type of noncarbonaceous chondrite. Palme and O'Neill (2004) also suggested that Earth's Mg/Si ratio is best matched, with a plausible proportion of Si sequestration into the core, by carbonaceous chondrites. For Mars, the most widely cited model (Dreibus and Wänke, 1985; Wänke and Dreibus, 1994) postulates a 35 wt.% contribution of CI carbonaceous chondrite-like matter; the other 65 wt.% being a reduced material akin to enstatite chondrites.

The term carbonaceous, as it is entrenched in the cosmochemical literature, is “somewhat of a misnomer” (Krot et al., 2004). Many “carbonaceous” chondrites are far from carbon-rich (Jarosewich, 1990; Pearson et al., 2006). However, the carbonaceous chondrites are distinctive, and similar amongst themselves, in various ways (including some to be adduced in this paper). As enumerated by Krot et al. (2004); (cf. Weisberg et al., 2006), “carbonaceous” characteristics include:  $^{16}\text{O}$ -rich oxygen isotopic composition (except in the case of CI); CI-or-higher mean ratio of refractory elements to the major lithophile element Si; relatively high abundance of refractory inclusions (except in CI); and high matrix/chondrule abundance ratio. Henceforward in this paper, the word carbonaceous will be used in that strict, meteoritics-customary sense.

For the Ti, Cr and Ni isotopic ratio anomalies exploited here, the variations observed are far too great to be the result of mass fractionation, so they probably reflect incomplete, and/or impermanent, mixing of stellar-nucleosynthetic ejecta (e.g., Dauphas et al., 2010; Leya et al., 2008; Qin et al., 2011). As reviewed by Dauphas et al. (2010) and Qin et al. (2011), neutron-rich isotopes with masses near that of iron are produced in Type Ia and II supernovae, but

\* Tel.: +1 310 825 3202; fax: +1 310 206 3051.

E-mail address: [pwarren@ucla.edu](mailto:pwarren@ucla.edu).

the detailed origin of these variations among, and within, meteorites is far from clear. The notion of impermanent mixing stems from [Trinquier et al. \(2009\)](#), who found, by normalizing to the  $^{49}\text{Ti}/^{47}\text{Ti}$  ratio, a correlation between  $^{46}\text{Ti}$  and  $^{50}\text{Ti}$ , which have different nucleosynthetic origins. These authors suggest that the protosolar molecular cloud may have once been well mixed, and invoke subsequent thermal processing to cause selective destruction of thermally unstable, isotopically anomalous presolar components. [Dauphas et al. \(2010\)](#) and [Qin et al. \(2011\)](#) have shown that enrichments in  $^{54}\text{Cr}$  are linked, in the CI1 Orgueil (and probably also the CM2 Murchison), with presolar Cr-oxide grains, most likely spinels, of order 10–100 nm in size. [Trinquier et al. \(2009\)](#) also found remarkable heterogeneity in  $\varepsilon^{50}\text{Ti}$ , mainly between chondrules and CAI (calcium-aluminum-rich inclusions), within the CV3 Allende.

The origin of the  $\Delta^{17}\text{O}$  diversity remains especially controversial ( $\Delta^{17}\text{O} \equiv \delta^{17}\text{O} - 0.52 \delta^{18}\text{O}$ ; where 0.52 is the slope of kinetic mass fractionation, including the Terrestrial Fractionation Line, TFL). Models range from episodic in-mixing of different reservoirs of stellar-nucleosynthetic origin (with perhaps a temporal trend toward higher  $\Delta^{17}\text{O}$ : [Wasson, 2000](#)), to “self shielded” ultraviolet photodissociation of CO, either in the parent molecular cloud ([Yurimoto and Kuramoto, 2004](#)) or within the solar nebula (e.g., [Lyons and Young, 2005](#); cf. [Clayton, 2008](#)). Presolar grains are trace components and rarely feature  $^{16}\text{O}$  enrichment ([Nittler, 2003](#)), so origin of the  $\Delta^{17}\text{O}$  diversity was clearly not tied to presolar nanoparticles of the type found by [Zinner et al. \(2005\)](#) (cf. [Dauphas et al., 2010](#)). The role of presolar, supernova-derived grains as original carriers of the correlated (see below) Ti, Cr and Ni isotopic anomalies warrants intense future study. One plausible model ([Qin et al., 2011](#)) postulates that grains from a Type II supernova were injected into the mature solar nebula, too late to become fully homogenized within the nebula. If the abundance of such grains varied in a systematic way, e.g., heliocentrically, they might track with and reflect a heliocentric compositional gradient (such as in  $\Delta^{17}\text{O}$ ) even if they were not the cause of it. In any case, like  $\Delta^{17}\text{O}$ , the  $\varepsilon^{50}\text{Ti}$ ,  $\varepsilon^{54}\text{Cr}$ , and  $\varepsilon^{62}\text{Ni}$  anomalies clearly are not primarily due to kinetic-molecular mass fractionation, and thus potentially provide important insight regarding planetary-material pedigree.

Existing meteorite classification schemes ([Krot et al., 2004](#); [Weisberg et al., 2006](#)) regard the carbonaceous chondrites as one of several top-level subdivisions of chondritic (primitive, undifferentiated) planetary material. At the same taxonomic level are four other subdivisions of chondrites, comprising the large ordinary (OC) and enstatite (EC) clans, as well as the rarer R (Rumuruti-like) and K (Kakangari-like) chondrite groups. Most of the ungrouped chondrites, as listed by [Krot et al. \(2004; their Table 1\)](#), are of carbonaceous affinity. This paper will show that a variety of recent high precision stable-isotopic measurements, when viewed in aggregate, suggest that a more apt classification has a top-level division between carbonaceous chondrites and all other chondrites. The stable-isotopic data also place rigorous limits on the proportions of carbonaceous chondritic matter in the Earth and Mars. Realistically, the planets formed as mixtures of various precursor materials, and even individually those precursors were not likely a close match with any known chondrite. Nonetheless, clear evidence now exists regarding which general type of material dominated the mix.

## 2. Data sources

This work exploits a wealth of recent high-precision analyses from several excellent teams of analysts. Titanium isotopic data are from just three sources: [Leya et al. \(2008\)](#), [Trinquier et al. \(2009\)](#), and, for lunar samples only, [Zhang et al. \(2011\)](#). Many of the data of [Trinquier et al. \(2009\)](#) were obtained as replicates at two separate labs, with good agreement between the two sets of results. Chromium isotopic data are taken from [Bogdanovski and Lugmair \(2004\)](#), [Yamashita et al. \(2005\)](#), [Shukolyukov and Lugmair \(2006a,b\)](#), [Ueda et al. \(2006\)](#),

[Trinquier et al. \(2007, 2008\)](#), [Yin et al. \(2009\)](#), [de Leuw et al. \(2010\)](#), [Qin et al. \(2010a,b\)](#), [Shukolyukov et al. \(2011\)](#), and especially, as the main source of bulk-ureilite measurements, [Yamakawa et al. \(2010\)](#). Nickel isotopic data are taken from [Regelous et al. \(2008\)](#), [Dauphas et al. \(2008\)](#) and [Quitte et al. \(2010\)](#). The Ni isotopic data of [Bizzarro et al. \(2007\)](#) are problematical ([Dauphas et al., 2008](#)) and were not utilized in this work. Oxygen isotopic data are taken mainly from an extensive compilation of data from the Clayton-Mayeda team (e.g., [Clayton et al., 1976; 1991; Clayton and Mayeda, 1988, 1996](#)). Clayton's data are augmented by a few more recent analyses, including seven carbonaceous chondrite analyses by [Yin et al. \(2009\)](#), plus seven analyses of Northwest Africa (NWA) ureilites listed in the *Meteoritical Bulletin* but otherwise unpublished. The graphs in this paper show averages for each meteorite type, except where significant stable-isotopic heterogeneity is manifest within the meteorite type; i.e., except for carbonaceous chondrites and ureilites. For those types, the plotted data instead consist of data pairs (whole-rock analyses) available from individual meteorites.

## 3. Ureilites: An exceptionally revealing class of achondrite

Among differentiated meteorites, the ureilites require special attention because they have diverse oxygen isotopic compositions ([Clayton and Mayeda, 1988](#)) that correlate with their silicate  $mg$  ( $\equiv \text{MgO}/(\text{MgO} + \text{FeO})$ ) ratios ([Downes et al., 2008; Mittlefehldt et al., 1998](#)). There is a general consensus that most, if not all, ureilites formed as anatectic (partial melting) mantle restites (e.g., [Goodrich et al., 2007; Kita et al., 2004; Takeda, 1987; Warren and Huber, 2006](#)). Ureilites have remarkably high bulk carbon contents: average 3 wt.%. Only CI chondrites are more C-rich. It has long been customary to assume that ureilite traits such as high bulk carbon contents and diverse,  $^{16}\text{O}$ -rich oxygen isotopic compositions imply a link with the carbonaceous chondrites (e.g., [Berkley et al., 1980; Goodrich et al., 2007; Kita et al., 2004; Singletary and Grove, 2006; Takeda, 1987; Vdovykin, 1970; Wasson et al., 1976](#)). But as this paper will review, a variety of stable-isotopic constraints ([Trinquier et al., 2009; Yamakawa et al., 2010](#), have been especially revealing) tell a very different story.

In using isotopes of Ti, Cr and Ni, ideally we would like to know the accretionary component(s) that dominantly contributed each of these elements. The mineralogy of ureilites, based on many separate samples, has been reviewed by, e.g., [Downes et al. \(2008\); Mittlefehldt et al. \(1998\)](#). Apart from their carbon-dominated interstitial areas (so-called “veins”), and their distinctive late reduction rims, ureilites are essentially pure olivine + pyroxene. Ureilite chromium is hosted overwhelmingly in the major minerals olivine and pyroxene. The situation is less clear for titanium, but its main host is probably pyroxene. Ti-rich phases such as ilmenite, ulvöspinel or armalcolite are unknown from non-polymict ureilites. In contrast, nickel in ureilites is hosted mainly in interstitial (“vein”) material. Ureilite bulk-rock Ni averages  $\sim 1250 \mu\text{g/g}$  and ranges from 230 to 2800  $\mu\text{g/g}$  ([Warren and Huber, 2006](#)). According to [Gabriel \(2009\)](#) (cf. [Gabriel and Pack, 2008](#)) ureilite olivines contain only 16–83  $\mu\text{g/g}$  Ni, and ureilite pyroxenes less than 26  $\mu\text{g/g}$ , while the metals of the interstitial areas generally contain 40,000–50,000  $\mu\text{g/g}$ . Thus, the current ureilite host setting for Ni (metals) is very different from the host setting for Cr (silicates; probably also true of Ti); so the full set of observed ureilite isotopic peculiarities (versus, e.g., carbonaceous chondrites) cannot be linked to any single minor component.

## 4. A fundamental dichotomy of planetary materials

### 4.1. Chromium and titanium isotopes

On a plot of  $\varepsilon^{50}\text{Ti}$  vs.  $\varepsilon^{54}\text{Cr}$  ([Fig. 1](#); cf. [Trinquier et al., 2009](#)), the carbonaceous chondrites plot in a distinct field, well separated from all other plotted material types, including ordinary (LL, L and H) chondrites, EH enstatite chondrites, and a wide range of differentiated materials that

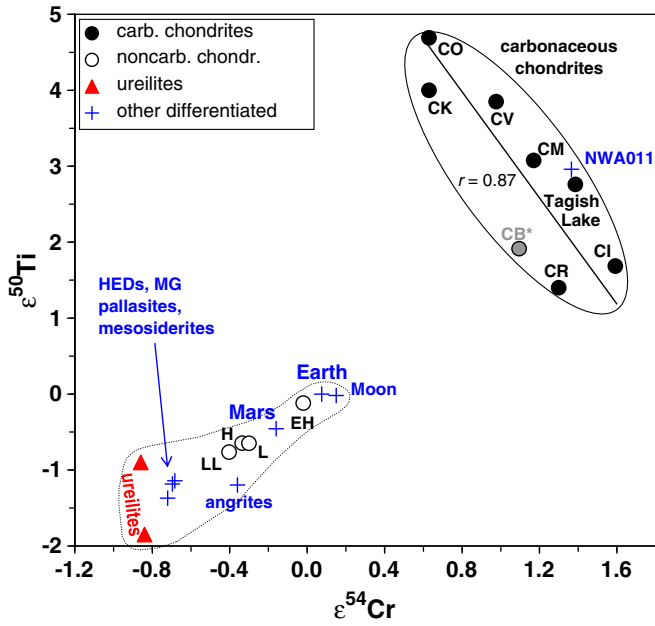


**Fig. 1.** Stable isotopes in planetary materials:  $\epsilon^{54}\text{Cr}$  vs.  $\epsilon^{50}\text{Ti}$ . For carbonaceous chondrites and ureilites, the plotted data consist of data pairs (whole-rock analyses) available from individual meteorites, except in the case of the CB carbonaceous chondrite group. Since no CB has been analyzed for both  $\epsilon^{54}\text{Cr}$  and  $\epsilon^{50}\text{Ti}$ , the plotted “CB\*” point is based on  $\epsilon^{54}\text{Cr}$  for a different CB (Shukolyukov and Lugmair, 2006a) from the two CBs that (averaged) provide the  $\epsilon^{50}\text{Ti}$  datum (Trinquier et al., 2009). The two ureilites that have been analyzed for both  $\epsilon^{50}\text{Ti}$  and  $\epsilon^{54}\text{Cr}$  are ALH 77257 and NWA 2376 (Leya et al., 2008; Trinquier et al., 2009; Ueda et al., 2006; Yamakawa et al., 2010).

includes the Earth, its Moon and Mars. In addition to the wide gap separating the carbonaceous chondrites from the other materials, note that the carbonaceous chondrites show a significant trend,  $r=0.87$  (or 0.82 including the relatively uncertain “CB\*” point), and the slope of this trend is approximately orthogonal to the rough trend of the “other” field. The carbonaceous trend is also approximately orthogonal to a vector that would extend from the carbonaceous chondrite field toward the other field. Thus, no realistic extension of the carbonaceous chondrite isotope-compositional distribution can be expected to incorporate the other materials.

4.2. Chromium and oxygen

Fig. 2 shows  $\epsilon^{54}\text{Cr}$  plotted vs.  $\Delta^{17}\text{O}$  (cf. Fig. 3 of Qin et al., 2010b). Again, the carbonaceous chondrites plot in a distinct field, well separated from the field within which cluster almost all other plotted material types, including ordinary (LL, L and H) chondrites, enstatite chondrites (both EL and EH), R chondrites, and a wide range of differentiated materials that includes the Earth, its Moon and Mars. The carbonaceous chondrites show a clearly significant correlation,  $r=0.92$  (or 0.91 including the relatively uncertain “CB\*” point). In this case, the configuration of the “other” field suggests a trend that roughly parallels the carbonaceous correlation. Admittedly, without the single R chondrite point, and/or without the ureilites, this trend would disappear. Still, a vector between the center of the carbonaceous chondrite field and the center of the other field would again be approximately orthogonal to the carbonaceous trend; and thus no realistic extension of the carbonaceous chondrite distribution can be expected to incorporate the other materials.

4.3. Chromium and nickel

Like oxygen, titanium and chromium, nickel shows considerable isotopic diversity among planetary materials. The overall pattern on a plot of  $\epsilon^{62}\text{Ni}$  vs.  $\epsilon^{54}\text{Cr}$  is a positive correlation (Fig. 3; cf. analogous

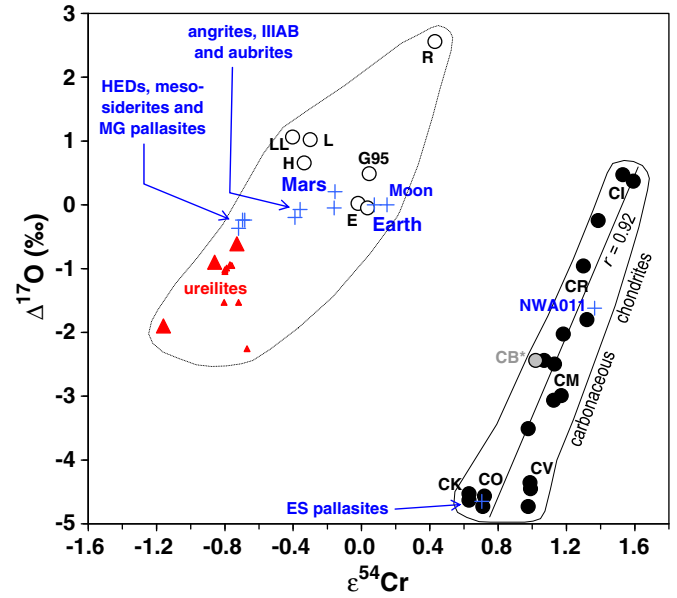


**Fig. 2.** Stable isotopes in planetary materials:  $\epsilon^{54}\text{Cr}$  vs.  $\Delta^{17}\text{O}$ . Symbols as for Fig. 1, except among ureilite data, smaller symbols represent diverse clasts from the Almahata Sitta polymict ureilite (Qin et al., 2010b). The three bulk ureilites that have been analyzed for both  $\epsilon^{54}\text{Cr}$  and  $\Delta^{17}\text{O}$  are ALH 77257, MET 78008, and Y-791538. For carbonaceous chondrites and ureilites, the plotted data consist of data pairs (whole-rock analyses) available from individual meteorites, except in the case of the CB group. Since no CB has been analyzed for both  $\epsilon^{54}\text{Cr}$  and  $\Delta^{17}\text{O}$ , the plotted “CB\*” point is based on  $\epsilon^{54}\text{Cr}$  for a different CB (Shukolyukov and Lugmair, 2006b) from the two CBs that (averaged) provide the  $\Delta^{17}\text{O}$  datum. “G95” is the unusual chondrite GRO 95511 (see text).

diagrams, based on smaller data sets, in Bizzarro et al., 2007; Regelous et al., 2008; however, as mentioned previously, the  $\epsilon^{62}\text{Ni}$  data of Bizzarro et al. are not used in this work). All five of the different analyzed carbonaceous chondrite groups are at the neutron-rich (in terms of  $\epsilon^{62}\text{Ni}$  and  $\epsilon^{54}\text{Cr}$ ) end of the trend. The noncarbonaceous

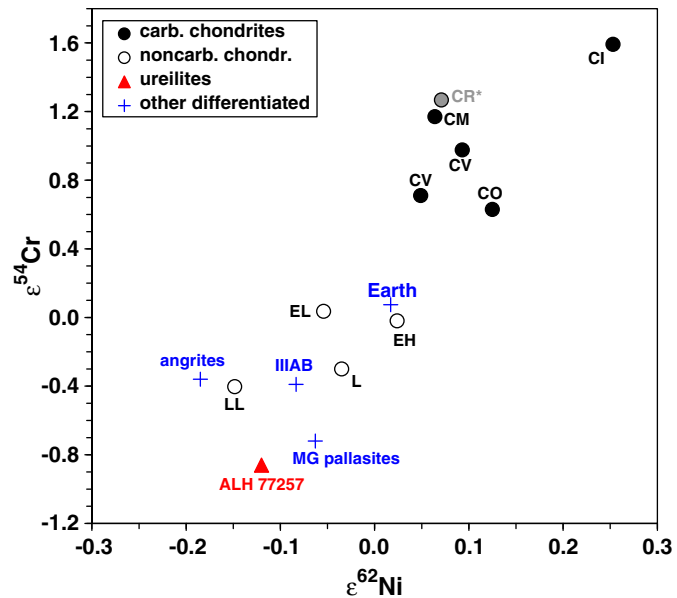


**Fig. 3.** Stable isotopes in planetary materials:  $\epsilon^{62}\text{Ni}$  vs.  $\epsilon^{54}\text{Cr}$ . For carbonaceous chondrites and ureilites, the plotted data consist of data pairs (whole-rock analyses) available from individual meteorites, except in the case of the CR group. Since no CR has been analyzed for both  $\epsilon^{62}\text{Ni}$  and  $\epsilon^{54}\text{Cr}$ , the plotted “CR\*” point is based on  $\epsilon^{62}\text{Ni}$  for a different CR (Regelous et al., 2008) from the three CRs that (averaged) provide the  $\epsilon^{54}\text{Cr}$  datum (Qin et al., 2010a; Trinquier et al., 2007; Yin et al., 2009). Although only one ureilite, ALH 77257, has been analyzed for both  $\epsilon^{62}\text{Ni}$  and  $\epsilon^{54}\text{Cr}$ , three others (Quitte et al., 2010) have  $\epsilon^{62}\text{Ni}$  of  $-0.60$  to  $0.07$  ( $\pm 0.48$ ).

chondrite groups are clustered toward the opposite end. Differentiated planetary materials, shown by crosses, tend to plot in the same low  $\epsilon^{62}\text{Ni}$ , low  $\epsilon^{54}\text{Cr}$  region. The one ureilite (ALH 77257) that has been analyzed for both  $\epsilon^{62}\text{Ni}$  and  $\epsilon^{54}\text{Cr}$  (Quitte et al., 2010; Ueda et al., 2006) plots at the extreme low  $\epsilon^{62}\text{Ni}$ , low  $\epsilon^{54}\text{Cr}$  end of the trend. That is, the opposite end from the carbonaceous chondrites.

## 5. Discussion

The distribution of the planetary materials on Figs. 1 and 2 is strongly bimodal, with two obviously distinct clusters for the carbonaceous versus noncarbonaceous materials. As more analyses are acquired in the future, it will be interesting to see how well this isotope-compositional bimodality withstands growth in the compositional-petrological diversity of the analyzed materials. But already the bimodality appears undoubtedly significant, with profound implications. The high degree of bimodality suggests that the highest taxonomic division in meteorite/planetary classification should be between carbonaceous and noncarbonaceous materials (Fig. 4). Admittedly, the terms carbonaceous and noncarbonaceous are awkward and misleading (cf. Krot et al., 2004). As the bimodality becomes better understood, the community should seek to agree upon more apt terms for the two material varieties, or at least for “noncarbonaceous”.

The positions of Earth and Mars on Figs. 1 and 2 obviously suggest that both planets consist primarily of noncarbonaceous material, with a carbonaceous-chondritic component of less than 50%. Before developing a more quantitative treatment of this issue, some related topics also warrant discussion.

### 5.1. Exceptional samples do not conflate the isotopic clusters

The significance of the bimodality becomes slightly clearer through consideration of meteorites that are in some ways aberrant in their stable-isotopic characteristics. In Fig. 2, the Eagle Station pallasites (actually only “ES” itself has thus far been analyzed: Shukolyukov and Lugmair, 2006b) plot far from all other metal-rich differentiated materials, yet not at a random position; they plot within the narrow carbonaceous field. Humayun and Weiss (2011) found that siderophile

constraints also favor a carbonaceous-chondritic derivation for the ES pallasites. The metal-rich chondrite GRO 95551 (plotted in Fig. 2 as “G95”) superficially resembles CB (Bencubbin group) carbonaceous chondrites (Mason, 1997). However, Weisberg et al. (2001) concluded on the basis of oxygen and nitrogen isotopes as well as mineral composition data that GRO 95551 represents “a different nebular reservoir” from the CB group. The Cr data of Qin et al. (2010a) show that GRO 95551 plots far from all carbonaceous materials, but again, not randomly; it plots within the field of the noncarbonaceous materials. The basaltic achondrite NWA 011 has far higher  $\epsilon^{54}\text{Cr}$  (Bogdanovski and Lugmair, 2004) and  $\epsilon^{50}\text{Ti}$  (Trinquier et al., 2009, analyzed the NWA 2976 pair) than most other basaltic planetary materials. Yet in Figs. 1 and 2 ( $\Delta^{17}\text{O}$  from Floss et al., 2005, Yamaguchi et al., 2002), NWA 011 falls squarely within the range of the carbonaceous materials. In each of these cases, the isotopic results, despite being unusual, hold true to form in the sense that the aberrant compositions avoid the gap between the carbonaceous and noncarbonaceous material types; i.e., instead of reducing the gap, Eagle Station and NWA 011 plot squarely in the carbonaceous region, and GRO 95551 plots squarely in the noncarbonaceous region.

Ureilites arguably constitute the most revealing “exception”. Previously, based on their high bulk carbon contents and diverse, low- $\Delta^{17}\text{O}$  oxygen isotopic compositions, the ureilites were seen as related to carbonaceous chondrites (e.g., Berkley et al., 1980; Goodrich et al., 2007; Kita et al., 2004; Singletary and Grove, 2006; Takeda, 1987; Vdovykin, 1970; Wasson et al., 1976). Ureilites, and as yet no other known type of achondrite, display an approximately +1 slope on the classic (Clayton et al., 1973) oxygen isotopes diagram:  $\delta^{18}\text{O}$  vs.  $\delta^{17}\text{O}$ . However, roughly +1 slope on the  $\delta^{18}\text{O}$  vs.  $\delta^{17}\text{O}$  diagram is not exclusively linked with the anhydrous-carbonaceous (CO-CK-CV) groups of chondrites. Clayton et al. (1991) noted that the ordinary chondrites (OC; i.e., LL, L and H), viewed as a related set, also form a trend with slope  $\sim +1$ . Among carbonaceous chondrites, the groups that exhibit +1 slopes (CO-CK-CV) only contain from 0.03 to 0.54 wt.% carbon (Jarosewich, 1990). Among the chondrites, whether noncarbonaceous (Jarosewich, 1990; Warren, 2008) or carbonaceous (Jarosewich, 1990; Pearson et al., 2006), carbon content exhibits an anticorrelation with metamorphic-petrologic type.

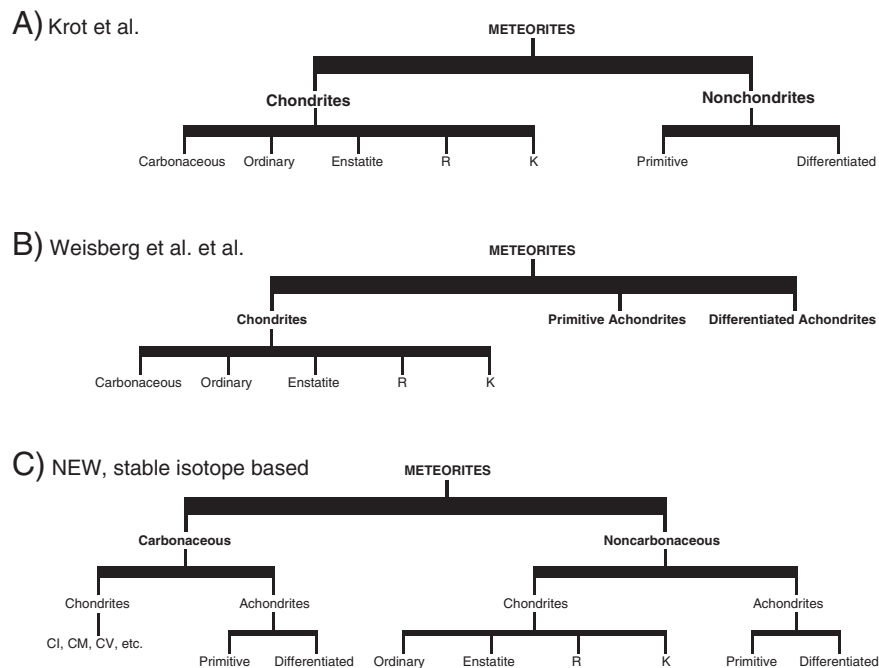


Fig. 4. Classification schemes for planetary materials, based on (A) Krot et al. (2004), (B) Weisberg et al. (2006), and (C) the stable-isotopic evidence discussed in this work. The new classification is adapted from older ones by addition of the carbonaceous vs. noncarbonaceous dichotomy.

As igneous restites, the ureilites are, in essence, petrologic type ~8 or 9. Extrapolated to type 8, the anticorrelation trend implies a C content of order 0.01 wt.%, i.e., too low by a factor of 100. That the carbonaceous chondrites, and not the noncarbonaceous, happen to include low metamorphic, C-rich types (all known noncarbonaceous chondrites are of petrologic type at least 3; most are types 5–6) is a weak argument for linkage with ureilites. In a warming planetesimal, carbon is prone to oxidation and loss as CO<sub>x</sub> gas (McSween and Labotka, 1993). Obviously this did not occur in the ureilites, presumably because the original ureilite parent body achieved a large size, and thus a sufficiently high internal pressure regime to stabilize solid C against oxidation, before it got very hot (Warren, 2008). The accretion, and retention, of carbon does not imply that the ureilite precursor matter was “carbonaceous” in the sense that has long been customary in meteorite classification. It is now apparent that ureilites, despite their high carbon and diversely low  $\Delta^{17}\text{O}$ , are actually not of carbonaceous pedigree. Again, it is impressive that the “exceptional” ureilite isotopic compositions not only plot in the general direction of the noncarbonaceous materials, in Figs. 1 and 3 the ureilites appear more “noncarbonaceous” than any other material.

Ureilites add considerably to the isotopic-compositional range of the noncarbonaceous class of materials, which includes the Earth. The identity, within uncertainty, of  $\Delta^{17}\text{O}$ ,  $\varepsilon^{54}\text{Cr}$  and  $\varepsilon^{50}\text{Ti}$  between Earth and the Moon (e.g., Zhang et al., 2011) thus grows even more remarkable, and difficult to reconcile with the popular Giant Impact hypothesis of lunar origin, except by invoking an initial homogenization of the Earth’s mantle + Moon system by turbulent mixing (Pahlevan et al., 2011).

## 5.2. Volatile depletion trends of the Earth and Mars

Allègre et al. (2001) and Palme and O’Neill (2004) have argued that the Earth’s volatile depletion trend is matched more closely by carbonaceous chondrites than by any type of noncarbonaceous chondrite. The Dreibus and Wänke (1985) (cf. Wänke and Dreibus, 1994) model for Mars postulates a 35 wt.% contribution of CI-like material; the other 65 wt.% being a reduced material akin to enstatite (E) chondrites. The stable-isotopic evidence (Figs. 1 and 2) renders the volatile-depletion resemblances to carbonaceous chondrites more enigmatic. However, in both the Allègre et al. (2001) and the Palme and O’Neill (2004) papers, although the authors note evidence suggesting that Earth’s building blocks underwent a similar variety of volatile-depletion processing as the carbonaceous chondrites, they emphasize the similarity of processing, and never claim that the building blocks were dominantly carbonaceous chondrites, per se.

Probably no single specific chondrite variety (group), much less any single variety known from the limited sampling provided by meteorites, was preponderant in the accretion of the Earth, or of Mars. However, it is worth noting that among noncarbonaceous chondrites, the enstatite chondrites, especially EH, feature relatively mild volatile depletions, not drastically unlike the carbonaceous chondrites (e.g., Fig. 3 in Allègre et al., 2001). Citing (inter alia) Earth’s high Fe-metal content, Javoy (1995) and Javoy et al. (2010) (cf. the early conjecture of Herndon, 1980) have argued that the bulk Earth accreted mainly from matter similar to EH-group chondrites. This model carries an implication that the final FeO content was raised, either through accretion of a lesser but important component of vastly more oxidized material (cf. Schönbächler et al., 2010), and/or by high-pressure redox; i.e., several percent of Fe-metal being oxidized to FeO while a commensurate proportion of SiO<sub>2</sub> gets reduced to (core) Si-metal. The latter process would also help to account for the Earth’s MgO/SiO<sub>2</sub> ratio, which (at least, as represented by the upper mantle) is high relative to any chondritic Mg/Si (e.g., Allègre et al., 2001; Palme and O’Neill, 2004), but especially relative to the enstatite chondrites (Jarosewich, 1990). In terms of

molybdenum isotopes, Earth, CI chondrites (Dauphas et al., 2002) and IAB/IIICD iron meteorites, all are similar, but various other differentiated meteorites and non-CI chondrites show positive anomalies (Burkhardt et al., 2010). For enstatite chondrites, no Mo data are yet available.

## 5.3. Constraints on the proportion of carbonaceous matter in the Earth and Mars

The positions of Earth and Mars on Figs. 1 and 2 show that both planets consist primarily of “noncarbonaceous” material, with a carbonaceous-chondritic component of less than 50%. To quantify these implied proportions, the lever rule can be applied with the planet modeled as a mixture of two end-members (Figs. 5 and 6). The aim is to constrain  $C/(C + NC)$ , where  $C$  is the planet’s carbonaceous component and  $NC$  is its noncarbonaceous component. A two-component mixing curve on a ratio-ratio diagram may be far from linear (Langmuir et al., 1978), but in this particular circumstance, because the concentrations of the elements involved (Cr, O and Ti) do not vary greatly among the materials in question (primitive chondritic materials and whole planets), the mixing curves must be close to linear.

For deriving a kind of upper limit on  $C/(C + NC)$ , the planet can be modeled as a blend of the carbonaceous-chondrite composition nearest to the planet  $C_{\text{near}}$  with the composition  $NC_{\text{farthest}}$  that is farthest away from  $C_{\text{near}}$  among the known noncarbonaceous materials. To make the limiting calculation more realistic, the noncarbonaceous end-member  $NC_{\text{far}}$  may be determined by excluding the two classes of material that have  $\Delta^{17}\text{O}$  outside the range (roughly 0 to +1) that, mixed with carbonaceous matter, can yield the planet’s observed  $\Delta^{17}\text{O}$  value (0‰ for Earth; practically the same, 0.2‰, for Mars); i.e., by excluding ureilites and R chondrites.

Another approach, aimed simply at a best rough estimate of the carbonaceous:noncarbonaceous mixing ratio without bias toward conservatism, is to estimate the most likely compositions of the two end members,  $C_{\text{est}}$  and  $NC_{\text{est}}$ . This approach involves enormous uncertainty,

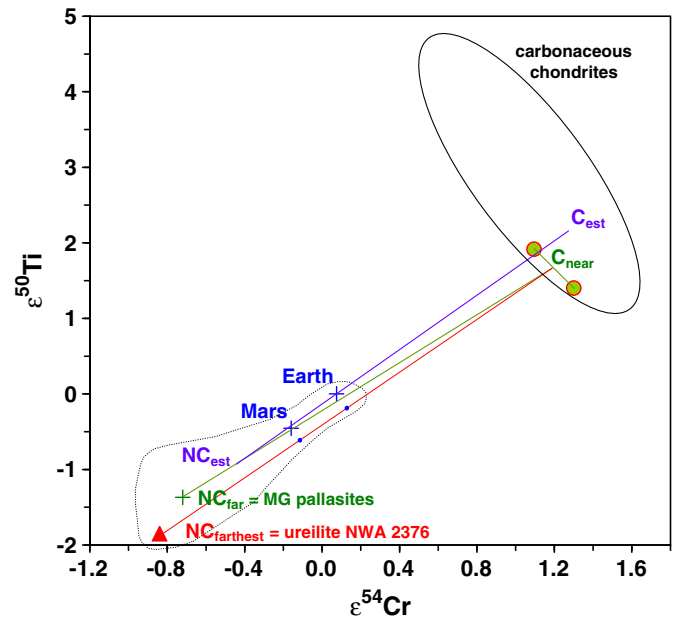


**Fig. 5.** Mass-balance (lever rule) models for the bulk compositions of Earth and Mars using  $\varepsilon^{54}\text{Cr}$  vs.  $\varepsilon^{50}\text{Ti}$ . The fields and choices for  $C_{\text{est}}$ ,  $NC_{\text{est}}$ ,  $C_{\text{near}}$ ,  $NC_{\text{far}}$  and  $NC_{\text{farthest}}$  (defined in text) are based on Fig. 1. For the mixing models, a slight extrapolation from the planet composition to the putative mixing line is necessary to finally arrive at a position for application of the lever rule. To minimize clutter in the diagram, these final short extrapolations are indicated only by small dots that show final extrapolated planet-assessment positions along the two mixing lines that pass farthest from the planet compositions (i.e., in this case, along the  $NC_{\text{farthest}}$  to  $C_{\text{near}}$  mixing line).

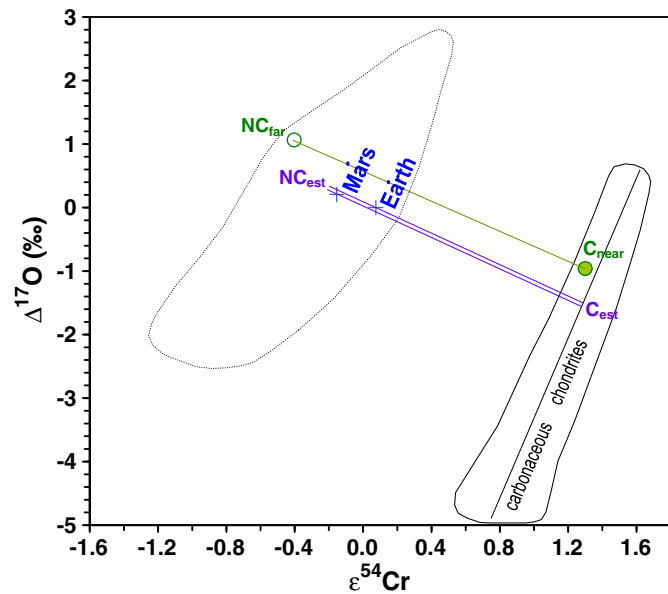


**Fig. 6.** Mass-balance (lever rule) models for the bulk compositions of Earth and Mars using  $\epsilon^{54}\text{Cr}$  vs.  $\Delta^{17}\text{O}$ . The fields and choices for  $C_{\text{est}}$ ,  $NC_{\text{est}}$ ,  $C_{\text{near}}$  and  $NC_{\text{far}}$  are based on Fig. 2. For the mixing models, a slight extrapolation from the planet composition to the putative mixing line is necessary to finally arrive at a position for application of the lever rule. To minimize clutter in the diagram, these final short extrapolations are indicated only by small dots that show final extrapolated planet-assessment positions along the two mixing lines that pass farthest from the planet compositions (i.e., in this case, along the  $NC_{\text{far}}$  to  $C_{\text{near}}$  mixing line).

but a very rough  $C/(C+NC)$  estimate (treated with due circumspection) may be preferable to no estimate. For a case of the noncarbonaceous data trend being far from parallel to the carbonaceous trend (Fig. 5), I estimate  $C_{\text{est}}$  and  $NC_{\text{est}}$  by simple averaging of the relevant data sets; which are taken to be, for  $C_{\text{est}}$ , the carbonaceous chondrite groups excluding those with  $\epsilon^{50}\text{Ti} > 3.5$  (i.e., excluding the anhydrous groups: CK, CO and CV); and for  $NC_{\text{est}}$ , all the separate noncarbonaceous material types, excluding the planets, the Moon, and also (as above) ureilites and R chondrites. For a case of the noncarbonaceous data and the carbonaceous data being distributed in subparallel trends (Fig. 6), I estimate  $C_{\text{est}}$  by finding the closest point to the planet's composition along the regression fit to the carbonaceous data set, and then extrapolate the line connecting those points to the  $NC_{\text{est}}$  composition, assumed to be half-way across the noncarbonaceous field.

The plot of  $\epsilon^{62}\text{Ni}$  vs.  $\epsilon^{54}\text{Cr}$  (Fig. 3) is not as useful for constraining the carbonaceous:noncarbonaceous mixing ratio. For many planetary material types (including Mars) combinations of reliable  $\epsilon^{62}\text{Ni}$  and  $\epsilon^{54}\text{Cr}$  data are not yet available, and the data that are available show a less organized distribution, with the Earth much farther from the CI chondrites than from all other carbonaceous materials. However, the  $\epsilon^{62}\text{Ni}$  vs.  $\epsilon^{54}\text{Cr}$  plot (Fig. 3) still suggests that Earth's  $NC/(C+NC)$ , is probably at least 50%; with compositional affinity to EH chondrites in particular.

**Table 1**  
Mass-balance (lever rule) modeling for the bulk compositions of Earth and Mars.

System used	Type of modeling	Results: carbonaceous/(carbonaceous+noncarbonaceous)	
		Earth	Mars
$\epsilon^{54}\text{Cr}$ vs. $\epsilon^{50}\text{Ti}$	Rough estimate	0.30	0.15
	Upper limit	0.43	0.30
	Extreme upper limit	0.49	0.36
$\epsilon^{54}\text{Cr}$ vs. $\Delta^{17}\text{O}$	Rough estimate	0.18	0.026
	Upper limit	0.32	0.18

Results from the modeling based on Figs. 5 and 6 are shown in Table 1. The rough, “estimated” constraints on the mixing ratio  $C/(C+NC)$  average 24% for Earth and 9% for Mars. The  $C_{\text{near}} + NC_{\text{far}}$  models yield upper limits for  $C/(C+NC)$  of 43% for Earth and 30% for Mars based on Fig. 5; and most importantly, upper limits of 32% for Earth and 18% for Mars based on Fig. 6. These “limits” are not absolute. The data are still sparse enough to leave some potential for slightly higher  $C/(C+NC)$ . But it seems clear that  $C/(C+NC)$  is much less than 50% for Earth, and less than 30% for Mars. Of course, purely from the perspective of the stable-isotopic evidence (Figs. 1–3), there is no requirement that  $C/(C+NC)$  be greater than zero in either planet, nor that Mars has a smaller  $C/(C+NC)$  than Earth. Over-specific models for planets as mixtures of the known chondrites should be regarded with caution, but if EH-like material dominated the Earth's noncarbonaceous component, as suggested by Javoy (1995; also Javoy et al., 2010), the proximity between Earth and EH in Figs. 1–3 is such that  $C/(C+NC)$  could, in principle, be very close to zero. A model for Mars as a mix of 85% ordinary chondrite plus 15% carbonaceous chondrite matter, i.e.,  $C/(C+NC) = 15\%$ , as suggested by Lodders and Fegley (1997), appears consistent with Figs. 1 and 2; except that, by favoring as the ordinary chondrite end member the relatively high- $\epsilon^{54}\text{Cr}$  H chondrites (cf. Hutchins et al., 2010), the Lodders and Fegley (1997) model implies (in terms of Figs. 1 and 2) a slightly smaller  $C/(C+NC)$  of about 8–13%.

#### 5.4. Possible implications for the spatial provenance of planetary materials?

There are relatively few differentiated meteorites of carbonaceous pedigree. Known examples are limited to the Eagle Station palasites and the NWA 011 basaltic achondrite. High petrologic type (i.e., thermally metamorphosed) chondrites are also relatively rare among the carbonaceous groups. It seems that carbonaceous planetesimals were in general less likely than noncarbonaceous planetesimals to undergo major heating. Such a pattern would be consistent with the common assumption (e.g., Wood, 2005) that the carbonaceous planetesimals tended to accrete at greater radial distance from the Sun.

Another common assumption (e.g., Bizzarro et al., 2007; Qin et al., 2010a) is that all the primitive planetary materials (chondrites) formed in the inner solar system. The source of most chondrites in terms of the mature solar system is surely the asteroid belt, at 2–4 AU, between Mars and Jupiter. Compositional diversity among the chondrites probably developed largely as an effect of temporally episodic accretion of the solar nebula (de Leuw et al., 2010; Wasson, 2000). However, the pattern of compositional bimodality in Figs. 1 and 2 is so pronounced, it suggests a model of binary-divergent origins. In the context of the early solar system, one obvious and fundamental potential divergence between two modes of origin is spatial, between the inner solar system (sunward relative to Jupiter) and the outer solar system. The location of the “snow line” in a mature protoplanetary nebula is believed to be well inside of Jupiter (Garaud and Lin, 2007; Kennedy and Kenyon, 2008; Lacar et al., 2006), and many of the carbonaceous chondrites (CK, CO and CV) are nearly anhydrous. However, the snow line may not have been as simple as commonly portrayed in nebular models. In the judgment of Wood (2005; his Fig. 2), all of the carbonaceous chondrites (or specifically, the groups CI, CM, CR, CO and CV) formed beyond the snow line; and even the ordinary chondrites formed partially beyond it. The only known orbit for a carbonaceous chondrite, the CI Orgueil, is most closely matched by the orbits of Jupiter-family comets (Gounelle et al., 2006). From the perspective of Figs. 1 and 2, it is hard to believe that the CI and CM carbonaceous chondrites could be products of the outer solar system, as suggested by Gounelle et al. (2008) (cf. Weissman et al., 2002), and yet the other kinds of carbonaceous chondrite come from the inner solar system, with the noncarbonaceous chondrites and nearly all of the differentiated materials. Going beyond Gounelle et al. (2008), I

speculate that if any of the carbonaceous chondrites originally accreted in the outer solar system, then most likely all carbonaceous chondrites originally accreted in the outer solar system. Walsh et al. (2011) (cf. Levison et al., 2009) have inferred that as a consequence of radial migration and mass growth of the giant planets, the belt region (today's meteorite source region) underwent a complex evolution that culminated in a significant inward migration of planetesimals from the outer solar system into the belt (mainly the outer belt) region.

## 6. Conclusions

1. The striking bimodality exhibited by planetary materials on the  $\epsilon^{50}\text{Ti}$  vs.  $\epsilon^{54}\text{Cr}$  and  $\Delta^{17}\text{O}$  vs.  $\epsilon^{54}\text{Cr}$  diagrams suggests that the highest taxonomic division in meteorite/planetary classification should be between carbonaceous and noncarbonaceous materials.
2. As the origin of the bimodality becomes better understood, the community should seek to eventually agree upon more apt terms for the two material varieties. The terms carbonaceous and noncarbonaceous are over-simplistic and even misleading (cf. Krot et al., 2004). The bimodality may represent an extreme manifestation of heterogeneous accretion within the protoplanetary disk, but if my speculation is correct, apt terms might be (or connote) inner solar system, to replace noncarbonaceous, and outer solar system, to replace carbonaceous.
3. Applying the lever rule to extrapolate from the  $\epsilon^{50}\text{Ti}$  vs.  $\epsilon^{54}\text{Cr}$  and  $\Delta^{17}\text{O}$  vs.  $\epsilon^{54}\text{Cr}$  diagrams, the carbonaceous/(carbonaceous + noncarbonaceous) mixing ratio  $C/(C+NC)$  is most likely (very roughly) 24% for Earth and 9% for Mars. Estimated upper limits for  $C/(C+NC)$  are 32% for Earth and 18% for Mars.
4. If the Earth is modeled as the equivalent of a single noncarbonaceous component (admittedly a great oversimplification), EH chondrites yield the closest fit to the stable-isotopic data. Dominance of EH-like material would also help to account for the relatively mild volatile depletions that would otherwise suggest a carbonaceous pedigree.

## Acknowledgments

I thank H. Palme and Anonymous for insightful, constructive reviews; Editor R. W. Carlson for additional helpful suggestions; and A. E. Rubin and especially J. T. Wasson for helpful advice. This work was supported by NASA grants NNX09AE31G and NNX09AM65G.

## References

Allège, C., Manhès, G., Lewin, E., 2001. Chemical composition of the Earth and the volatility control on planetary genetics. *Earth Planet. Sci. Lett.* 185, 49–69.

Berkley, J.L., Taylor, G.J., Keil, K., Harlow, G.E., Prinz, M., 1980. The nature and origin of ureilites. *Geochim. Cosmochim. Acta* 44, 1579–1597.

Bizzarro, M., Ulfbeck, D., Trinquier, A., Thrane, K., Connelly, J.N., Meyer, B.S., 2007. Evidence for a late supernova injection of  $^{60}\text{Fe}$  into the protoplanetary disk. *Science* 316, 1178–1181.

Bogdanovski, O., Lugmair, G.W., 2004. Manganese-chromium isotope systematics of basaltic achondrite Northwest Africa 011. *Lunar Planet. Sci.* 35 (abstract #1715).

Burkhardt, C., Kleine, T., Oberli, F., Bourdon, B., 2010. The molybdenum isotopic composition of meteoritic metals: evidence for planetary scale isotope heterogeneity of the solar nebula. *Lunar Planet. Sci.* 41 (abstract #2131).

Clayton, R.N., 2008. Oxygen isotopes in the early Solar System — a historical perspective. *Rev. Mineral. Geochem.* 68, 5–14.

Clayton, R.N., Mayeda, T.K., 1988. Formation of ureilites by nebular processes. *Geochim. Cosmochim. Acta* 52, 1313–1318.

Clayton, R.N., Mayeda, T.K., 1996. Oxygen isotope studies of achondrites. *Geochim. Cosmochim. Acta* 60, 1999–2017.

Clayton, R.N., Grossman, L., Mayeda, T.K., 1973. A component of primitive nuclear composition in carbonaceous meteorites. *Science* 182, 485–488.

Clayton, R.N., Onuma, N., Mayeda, T.K., 1976. A classification of meteorites based on oxygen isotopes. *Earth Planet. Sci. Lett.* 30, 10–18.

Clayton, R.N., Mayeda, T.K., Goswami, J.N., Olsen, E.J., 1991. Oxygen isotope studies of ordinary chondrites. *Geochim. Cosmochim. Acta* 55, 2317–2337.

Dauphas, N., Marty, B., Reisberg, L., 2002. Molybdenum nucleosynthetic dichotomy revealed in primitive meteorites. *Astrophys. J.* 569, L139–L142.

Dauphas, N., Cook, D.L., Sacarabany, A., Froehlich, C., Davis, A.M., Wadhwa, M., Pourmand, A., Rauscher, T., Gallino, R., 2008. Iron 60 evidence for early injection and efficient mixing of stellar debris in the protosolar nebula. *Astrophys. J.* 686, 560–569.

Dauphas, N., Remusat, L., Chen, J.H., Rosko, M.M., Papanastassiou, D.A., Stodolna, J., Guan, Y., Ma, C., 2010. Neutron-rich chromium isotope anomalies in supernova nanoparticles. *Astrophys. J.* 720, 1577.

de Leuw, S., Papanastassiou, D., Wasson, J.T., 2010. Chromium isotopes in chondrites and the heterogeneous accretion of the solar nebula abstract #2703 *Lunar Planet. Sci.* 41 (abstract #2703).

Downes, H., Mittlefehldt, D.W., Kita, N., Valley, J.W., 2008. Evidence from polymict ureilite meteorites for a disrupted and re-accreted single ureilite parent asteroid gardened by several distinct impactors. *Geochim. Cosmochim. Acta* 72, 4825–4844.

Dreibus, G., Wänke, H., 1985. Mars, a volatile-rich planet. *Meteoritics* 20, 367–381.

Floss, C., Taylor, L.A., Promprated, P., Rumble III, D., 2005. Northwest Africa 011: a “eucritic” basalt from a non-eucrite parent body. *Meteorit. Planet. Sci.* 40, 343–360.

Gabriel, A.D., 2009. Origin and Evolution of Ureilite Vein Metal – Fe, Ni, Co and Ni Isotope Systematics of Ureilite Vein Metal and Ureilite Silicates. Doctoral thesis, Univ. Göttingen, 215 pp.

Gabriel, A.D., Pack, A., 2008. Fe, Co and Ni in ureilite metal and silicates. *Lunar Planet. Sci.* 39 (abstract #1391).

Garau, P., Lin, D.N.C., 2007. The effects of internal dissipation and surface irradiation on the structure of disks and the location of the snow line around Sun-like stars. *Astrophys. J.* 654, 606–624.

Goodrich, C.A., Van Orman, J.A., Wilson, L., 2007. Fractional melting and smelting on the ureilite parent body. *Geochim. Cosmochim. Acta* 71, 2876–2895.

Gounelle, M., Spurný, P., Bland, P.A., 2006. The atmospheric trajectory and orbit of the Orgueil meteorite. *Meteorit. Planet. Sci.* 41, 135–150.

Gounelle, M., Morbidelli, A., Bland, P.A., Spurný, P., Young, E.D., Sephton, M., 2008. Meteorites from the outer solar system? In: Barucci, M.A., Boehnhardt, H., Cruikshank, D.P., Morbidelli, A. (Eds.), *The Solar System Beyond Neptune*. Univ Arizona Press, pp. 525–541.

Herndon, J.M., 1980. The chemical composition of the interior shells of the Earth. *Proc. R. Soc. Lond.* A372, 149–154.

Humayun, M., Weiss, B.P., 2011. A common parent body for Eagle Station pallasites and CV chondrites. *Lunar Planet. Sci.* 42 (abstract #1507).

Hutchins, K., Agee, C.B., Draper, D.S., 2010. High pressure experiments yield insight into an early magma ocean on Mars. *Lunar Planet. Sci.* 41 (abstract #1525).

Jarosewich, E., 1990. Chemical analyses of meteorites: a compilation of stony and iron meteorite analyses. *Meteoritics* 25, 323–337.

Javoy, M., 1995. The integral enstatite chondrite model of the Earth. *Geophys. Res. Lett.* 22, 2219–2222.

Javoy, M., Kaminski, E., Guyot, F., Andraut, D., Sanloup, C., Moreira, M., Labrosse, S., Jambon, A., Agrinier, P., Davaille, A., Jaupart, C., 2010. The chemical composition of the Earth: enstatite chondrite models. *Earth Planet. Sci. Lett.* 293, 259–268.

Kennedy, G.M., Kenyon, S.J., 2008. Planet formation around stars of various masses: the snow line and the frequency of giant planets. *Astrophys. J.* 673, 502–512.

Kita, N.T., Ikeda, Y., Togashi, S., Liu, Y., Morishita, Y., Weisberg, M.K., 2004. Origin of ureilites inferred from a SIMS oxygen isotopic and trace element study of clasts in the Dar al Gani 319 polymict ureilite. *Geochim. Cosmochim. Acta* 68, 4213–4235.

Krot, A.N., Keil, K., Goodrich, C.A., Scott, E.R.D., Weisberg, M.K., 2004. Classification of meteorites. In: Davis, A.M. (Ed.), *Treatise on Geochemistry: Meteorites, Comets, Planets*, 1. Elsevier-Pergamon, Oxford, pp. 83–128.

Lacar, M., Podolak, M., Sasselov, D., Chiag, E., 2006. On the location of the snow line in a protoplanetary disk. *Astrophys. J.* 640, 1115–1118.

Langmuir, C.H., Vocke, R.D., Hanson, G.N., Hart, S.R., 1978. A general mixing equation with applications to Icelandic basalts. *Earth Planet. Sci. Lett.* 37, 380–392.

Levison, H.F., Bottke, W.F., Gounelle, M., Morbidelli, A., Nesvorný, D., Tsiganis, K., 2009. Contamination of the asteroid belt by primordial trans-Neptunian objects. *Nature* 460, 364–366.

Leya, I., Schoenbachler, M., Wiechert, U., Krahenbuhl, U., Halliday, A.N., 2008. Titanium isotopes and the radial heterogeneity of the solar system. *Earth Planet. Sci. Lett.* 266, 233–244.

Lodders, K., Fegley, B., 1997. An oxygen isotopic model for the composition of Mars. *Icarus* 126, 373–394.

Lyons, J.R., Young, E.D., 2005. CO self-shielding as the origin of oxygen isotope anomalies in the early solar nebula. *Nature* 435, 317–320.

Mason, B., 1997. GRO 95551 thin section description. *Antarct. Meteorit. Newsl.* 20 (2), 16.

McDonough, W.F., Sun, S.-S., 1995. The composition of the Earth. *Chem. Geol.* 120, 223–253.

McSween Jr., H.Y., Labotka, T.C., 1993. Oxidation during metamorphism of the ordinary chondrites. *Geochim. Cosmochim. Acta* 57, 1105–1114.

Mittlefehldt, D.W., McCoy, T.J., Goodrich, C.A., Kracher, A., 1998. Non-chondritic meteorites from asteroidal bodies. *Rev. Mineral.* 36, 41–4195.

Nittler, L.R., 2003. Presolar stardust in meteorites: recent advances and scientific frontiers. *Earth Planet. Sci. Lett.* 209, 259–273.

Pahlevan, K., Stevenson, D.J., Eiler, J.M., 2011. Chemical fractionation in the silicate vapor atmosphere of the Earth. *Earth Planet. Sci. Lett.* 301, 433–443.

Palme, H., O'Neill, H., St, C., 2004. Cosmochemical estimates of mantle composition. In: Carlson, R.W. (Ed.), *Treatise on Geochemistry: The Mantle and Core*, Volume 2. Elsevier-Pergamon, Oxford, pp. 1–38.

Pearson, V.K., Sephton, M.A., Franchi, I.A., Gibson, J.M., Gilmour, I., 2006. Carbon and nitrogen in carbonaceous chondrites: elemental abundances and stable isotopic compositions. *Meteorit. Planet. Sci.* 41, 1899–1918.

- Qin, L., Alexander, C.M., Carlson, R.W., Horan, M.F., Yokoyama, T., 2010a. Contributors to chromium isotope variation of meteorites. *Geochim. Cosmochim. Acta* 74, 1122–1145.
- Qin, L., Rumble, D., Alexander, C.M., Carlson, R.W., Jenniskens, P., Shaddad, M.H., 2010b. The chromium isotopic composition of Almahata Sitta. *Meteorit. Planet. Sci.* 45, 1771–1777.
- Qin, L., Nittler, L.R., Alexander, C.M., Wang, J., Stadermann, F.J., Carlson, R.W., 2011. Extreme  $^{54}\text{Cr}$ -rich nano-oxides in the CI chondrite Orgueil – implication for a late supernova injection into the solar system. *Geochim. Cosmochim. Acta* 75, 629–644.
- Quitte, G., Markowski, A., Latkoczy, C., Gabriel, A., Pack, A., 2010. Iron-60 heterogeneity and incomplete isotope mixing in the early solar system. *Astrophys. J.* 720, 1215–1224.
- Regelous, M., Elliott, T., Coath, C.D., 2008. Nickel isotope heterogeneity in the early solar system. *Earth Planet. Sci. Lett.* 272, 330–338.
- Righter, K., Drake, M.J., Scott, E., 2006. Compositional relationships between meteorites and terrestrial planets. In: Lauretta, D.S., McSween Jr., H.Y. (Eds.), *Meteorites and the Early Solar System II*. Univ Arizona Press, Tucson, pp. 19–52.
- Schönbächler, M., Carlson, R.W., Horan, M.F., Mock, T.D., Hauri, E.H., 2010. Heterogeneous accretion and the moderately volatile element budget of Earth. *Science* 328, 884–887.
- Shukolyukov, A., Lugmair, G.W., 2006a. Manganese-chromium isotope systematics of carbonaceous chondrites. *Earth Planet. Sci. Lett.* 250, 200–213.
- Shukolyukov, A., Lugmair, G.W., 2006b. The Mn–Cr isotope systematics in the ureilites Kenna and LEW85440. *Lunar Planet. Sci.* 37 (abstract #1478).
- Shukolyukov, A., Lugmair, G.W., Irving, A.J., 2011. Mn–Cr isotope systematics and excess of 54-Cr in metachondrite Northwest Africa 3133. *Lunar Planet. Sci.* 42 (abstract #1527).
- Singletary, S., Grove, T.L., 2006. Experimental constraints on ureilite petrogenesis. *Geochim. Cosmochim. Acta* 70, 1291–1308.
- Takeda, H., 1987. Mineralogy of Antarctic ureilites and a working hypothesis for their origin and evolution. *Earth Planet. Sci. Lett.* 81, 358–370.
- Trinquier, A., Bircck, J.-L., Allègre, C.J., 2007. Widespread  $^{54}\text{Cr}$  heterogeneity in the inner solar system. *Astrophys. J.* 655, 1179–1185.
- Trinquier, A., Bircck, J.-L., Allègre, C.J., Gopel, C., Ulfbeck, D., 2008.  $^{53}\text{Mn}$ – $^{53}\text{Cr}$  systematics of the early Solar System revisited. *Geochim. Cosmochim. Acta* 72, 5146–5163.
- Trinquier, A., Elliott, T., Ulfbeck, D., Coath, C., Krot, A.N., Bizzarro, M., 2009. Origin of nucleosynthetic isotope heterogeneity in the solar protoplanetary disk. *Science* 324, 374–376.
- Ueda, T., Yamashita, K., Kita, N., 2006. Chromium isotopic systematics of ureilite (abstract). NIPR Symp. Antarct. Meteorit. XXX, 117–118.
- Vdovykin, G.P., 1970. Ureilites. *Space Sci. Rev.* 10, 483–510.
- Walsh, K.J., Morbidelli, A., Raymond, S.N., O'Brien, D.P., Mandell, A.M., 2011. A low mass for Mars from Jupiter's early gas-driven migration. *Nature* 475, 206–209.
- Wänke, H., Dreibus, G., 1994. Chemistry and accretion history of Mars. *Philos. Trans. Phys. Sci. Eng.* 349, 285–293.
- Warren, P.H., 2008. A depleted, not ideally chondritic bulk Earth: the explosive-volcanic basalt loss hypothesis. *Geochim. Cosmochim. Acta* 72, 2217–2235.
- Warren, P.H., Huber, H., 2006. Ureilite petrogenesis: a limited role for smelting during anatexis and catastrophic disruption. *Meteorit. Planet. Sci.* 41, 835–849.
- Wasson, J.T., 2000. Oxygen-isotopic evolution of the solar nebula. *Rev. Geophys.* 38, 491–512.
- Wasson, J.T., Chou, C.-L., Bild, R.W., Baedeker, P.A., 1976. Classification of and elemental fractionation among ureilites. *Geochim. Cosmochim. Acta* 40, 1449–1450.
- Weisberg, M.K., Prinz, M., Clayton, R.N., Mayeda, T.K., Sugiura, N., Zashu, S., Ebihara, M., 2001. A new metal-rich chondrite grouplet. *Meteorit. Planet. Sci.* 36, 401–418.
- Weisberg, M.K., McCoy, T.J., Krot, A.N., 2006. Systematics and evaluation of meteorite classification. In: Lauretta, D.S., McSween Jr., H.Y. (Eds.), *Meteorites and the Early Solar System II*. Univ Arizona Press, Tucson, pp. 19–52.
- Weissman, P.R., Bottke Jr., W.F., Levison, H., 2002. Evolution of comets into asteroids. In: Bottke, W.F., Cellino, A., Paolicchi, P., Binzel, R.P. (Eds.), *Asteroids III*. Univ Arizona Press, pp. 669–686.
- Wood, J.A., 2005. The chondrite types and their origins. In: Krot, A.N., Scott, E.R.D., Reipurth, B. (Eds.), *Chondrites and the Protoplanetary Disk*, *Astronomical Society of Pacific Conference Series*, Vol. 247, pp. 953–971.
- Yamaguchi, A., Clayton, R.N., Mayeda, T.K., Ebihara, M., Oura, Y., Miura, Y.N., Hiramura, H., Misawa, K., Kojima, H., Nagao, K., 2002. A new source of basaltic meteorites inferred from Northwest Africa 011. *Science* 296, 334–336.
- Yamakawa, A., Yamashita, K., Makashima, A., Nakamura, E., 2010. Chromium isotope systematics of achondrites: chronology and isotopic heterogeneity of the inner solar system. *Astrophys. J.* 720, 150–154.
- Yamashita, K., Ueda, T., Nakamura, N., Kita, N., Heaman, L.M., 2005. Chromium isotopic study of mesosiderite and ureilite: evidence for  $\epsilon^{54}\text{Cr}$  deficit in differentiated meteorites (abstract). NIPR Symp. Antarct. Meteorit. XXIX, 100–101.
- Yin, Q.-Z., Yamashita, K., Yamakawa, A., Tanaka, B., Jacobsen, B., Ebel, D., Hutcheon, I.D., Nakamura, E., 2009.  $^{53}\text{Mn}$ – $^{53}\text{Cr}$  systematics of Allende chondrules and a  $^{54}\text{Cr}$ – $\Delta^{17}\text{O}$  correlation in bulk carbonaceous chondrites. *Lunar Planet. Sci.* 40 (abstract #2006).
- Yurimoto, H., Kuramoto, K., 2004. Molecular cloud origin for the oxygen isotope heterogeneity in the solar system. *Science* 305, 1763–1766.
- Zhang, J., Dauphas, N., Davis, A.M., 2011. Titanium isotope homogeneity in the Earth–Moon system: evidence for complete isotope mixing between the impactor and the protoEarth. *Lunar Planet. Sci.* 42 (abstract #1515).
- Zinner, E., Nittler, L.R., Hoppe, P., Gallino, R., Straniero, O., Alexander, C.M.O'D., 2005. Oxygen, magnesium and chromium isotopic ratios of presolar spinel grains. *Geochim. Cosmochim. Acta* 69, 4149–4165.